How to evaluate the cellular uptake of CPPs with fluorescence techniques: Dissecting methodological pitfalls associated to tryptophan-rich peptides

Quentin Seisel, François Pelletier, Sébastien Deshayes, Prisca Boisguérin

1 **How to evaluate the cellular uptake of CPPs with fluorescence techniques: dissecting methodological**
2 **pitfalls associated to tryptophan-rich peptides.**
3
4 Quentin Seisel, François Pelletier, Sébastien Deshayes, Prisca Boisguerin
5
6 Centre de Recherche de Biologie cellulaire de Montpellier, CNRS UMR 5237, Université Montpellier, 1919
7 Route de Mende, 34293 Montpellier Cedex 5, France.
8
10
11 **ABSTRACT**
12
13 Cell-penetrating peptides (CPP) are broadly recognized as efficient non-viral vectors for the internalization
14 of compounds such as peptides, oligonucleotides or proteins. Characterizing these carriers requires
15 reliable methods to quantify their intracellular uptake. Flow cytometry on living cells is a method of choice
16 but is not always applicable (e.g. big or polarized cells), so we decided to compare it to fluorescence
17 spectroscopy on cell lysates. Surprisingly, for the internalization of a series of TAMRA-labeled conjugates
18 formed of either cationic or amphipathic CPPs covalently coupled to a decamer peptide, we observed
19 important differences in internalization levels between both methods.
20   We partly explained these discrepancies by analyzing the effect of buffer conditions (pH, detergents)
21 and peptide sequence/structure on TAMRA dye accessibility. Based on this analysis, we calculated a
22 correction coefficient allowing a better coherence between both methods. However, an overestimated
23 signal was still observable for both amphipathic peptides using the spectroscopic detection, which could
24 be due to their localization at the cell membrane. Based on several *in vitro* experiments modeling events
25 at the plasma membrane, we hypothesized that fluorescence of peptides entrapped in the membrane
26 bilayer could be quenched by the tryptophan residues of close transmembrane proteins. During cell lysis,
27 cell membranes are disintegrated liberating the entrapped peptides and restoring the fluorescence,
28 explaining the divergences observed between flow cytometry and spectroscopy on lysates.
29   Overall, our results highlighted major biases in the fluorescently-based quantification of internalized
30 fluorescently-labeled CPP conjugates, which should be considered for accurate uptake quantification.
31
32
33

1. INTRODUCTION

Cell-penetrating peptides (CPPs) have the ability to cross cellular membranes, either alone or while transporting other molecular cargoes either covalently linked or non-covalently associated to them [1–3]. Work in the CPP area stemmed from the discovery that the third helix of the Antennapedia homeodomain (pAntp[43-58]) [4] and the transactivator of transcription of HIV-1 (Tat) [5,6] can cross biological membranes on their own. Following these findings, the number of peptides assigned to the CPP family has drastically increased within the last two decades [7–9]. CPPs have a great sequence diversity, but can nowadays be classified in three major classes: cationic (83%), amphipathic (44%) and hydrophobic (15%), some of them being part of several classes [10].

Backed by various experimental protocols, it is now largely accepted that CPPs can penetrate *via* energy-dependent routes (endocytosis) as well as *via* energy-independent pathways (direct translocation or transduction) [11]. Therefore, CPPs constitute excellent tools for promoting intracellular delivery of therapeutics even to organelles like mitochondria [12] or to bacteria [13]. The question of the internalization mechanism is fundamental for the selection of the adequate CPP for a distinct application or for the transport of a specific cargo.

The internalization efficiency of CPPs can easily be evaluated using fluorescently-based techniques such as flow cytometry or confocal microscopy, which are predominant in the literature: fluorophore-labeled CPP-conjugates are used to this extent [3]. Fluorescently-based analytical tools applied to CPPs have first been criticized because of the CPP cell-surface binding leading to an overestimation of the internalized CPP fraction by flow cytometry, as well as for their redistribution upon fixation of the cells for confocal microscopy [14]. To circumvent these pitfalls, enzymatic digestion should be performed to eliminate externally-sticking CPPs and microscopic imaging should be performed on living cells.

For a rapid screening and comparison of the internalization of different CPP-conjugates, flow cytometry is the most adequate method. However, in some cases this approach is not applicable for too large cells (e.g. cardiomyocytes) or for polarized epithelial cells (e.g. air-liquid interface culture) which cannot be separated by digesting enzymes due to tight junction formation. To evaluate the internalization of CPP-conjugates in polarized epithelial cells (for example in the context of cystic fibrosis) only quantitative fluorescence spectroscopy of cell lysates could be performed. Absolute quantification of CPP internalization by quantitative fluorescence spectroscopy converged with those obtained by mass spectrometry [15] and with those collected by flow cytometry but in a limited range of peptide/cell ratio [16].

One should also consider that fluorophore labeling of a CPP can have several impacts on cells affecting the interpretation of the fluorescence quantification. In details, Birch et al. (2017) has evaluated seven different fluorescence dyes coupled to the CPP penetratin and have clearly demonstrated that the different physico-chemical properties of the conjugates affect their cellular distribution and toxicity [17]. In particular, the mode of biomembrane interaction changed considerably upon fluorescence-labeling of the CPP penetratin with different dyes [18]. Fluorescence dye selection plays an important role for an exact CPP internalization without artefacts.

In the present study, we have coupled the cargo iCAL36 – a potent therapeutic peptide with cystic fibrosis application [19,20] – to a subset of different CPPs: Tat [21] (the most common used CPP), MPG (primary amphipathic peptide from our previous CPP screen [22,23]), C6M1 [24] (secondary amphipathic

peptide) and WRAP5 [25] (tryptophan and arginine-rich amphipathic peptide). The cellular internalization of these conjugates was evaluated by flow cytometry, fluorescence spectroscopy and confocal microscopy to compare the reliability and the robustness of these three methods for intracellular CPP detection. The mixed isomer 5(6)-carboxytetramethylrhodamine (TAMRA) was selected to follow CPP-conjugate internalization due to its strong fluorescent signal, its low membrane binding when conjugated to a peptide and its multiple biological applications [17]. Furthermore, TAMRA is known to have a relatively low sensitivity to photobleaching or solvatochromism compared to other fluorophores such as fluorescein [26,27].

Herein, we demonstrate that fluorescence intensity of the measured TAMRA-CPP-conjugates is a function of the CPP sequence as well as, when used, of the composition of the lysis buffer. Furthermore, we showed that TAMRA/TAMRA, TAMRA/lipid or TAMRA/tryptophan quenching could lead to over- or under-estimation of the occurring peptide internalization depending on the used screening method (flow cytometry *versus* fluorescence spectroscopy). Our results give an overview of possible pitfalls which could occur during the quantification of CPP uptake by fluorescence techniques. We will show that these biases especially concern peptides able of membrane destabilization and/or exhibiting high tryptophan content, such as secondary amphipathic CPPs.

2. MATERIALS AND METHODS

2.1. Peptide synthesis
Peptide synthesis was performed by LibertyBlue™ Microwave Peptide Synthesizer (CEM Corporation), an additional module of Discover™ (CEM Corporation) combining microwave energy at 2450 MHz to the fluorenylmethoxycarbonyl (Fmoc)/*tert*-butyl (*t*Bu) strategy. Peptide identity and purity was checked by LC-MS (Waters). Unlabeled and TAMRA-labeled peptides (**Table 1**) were used with a purity higher than 95% to ensure no differences due to different labeling efficiency.
For more details, see Supplementary Material.

Table 1: Sequences used in this study.

Name	ID	Sequences	MW [g/mol]	AA
iCAL36	36	ANSR**W**PTSII	1144.3	10
*iCAL36	*36	*****-ANSR**W**PTSII	1556.7	10
Tat-iCAL36	T36	GRKKRRQRRRPPQ-ANSR**W**PTSII	2843.6	23
*Tat-iCAL36	*T36	*****-GRKKRRQRRRPPQ-ANSR**W**PTSII	3256.1	23
MPG-iCAL36	M36	GALFLG**W**LGAAGSTMGA**W**SQPKKKRKV-ANSR**W**PTSII	3972.3	37
*MPG-iCAL36	*M36	*****-GALFLG**W**LGAAGSTMGA**W**SQPKKKRKV-ANSR**W**PTSII	4384.8	37
C6M1-iCAL36	C36	RL**W**RLL**W**RL**W**RRL**W**RLLR-ANSR**W**PTSII	3772.2	28
*C6M1-iCAL36	*C36	*****-RL**W**RLL**W**RL**W**RRL**W**RLLR-ANSR**W**PTSII	4184.7	28
WRAP5-iCAL36	W36	LLRLLR**WWW**RLLRLL-ANSR**W**PTSII	3230.9	25
*WRAP5-iCAL36	*W36	*****-LLRLLR**WWW**RLLRLL-ANSR**W**PTSII	3643.4	25

Footnote: ***** = TAMRA

2.2. Peptide solubilization

Peptide stock solutions were prepared at 500 µM in milliQ water (for *W36 2% of DMSO were added for solubilization purposes). After sonication for 5 min and centrifugation (5 min, 13,200 rpm), supernatant of the peptide solution was filtered (0.22 µm). Finally, peptide concentration was controlled by absorbance at 280 nm using a NanoDrop device (Thermo Scientific).

2.3. Cell culture

Human epithelial colorectal adenocarcinoma (Caco-2) cells were purchased from ATCC (HTB-37). Cells were maintained in DMEM 4.5 g/L glucose supplemented with UltraGlutamine (Lonza), 20% fetal bovine serum (FBS from PAA), 1% MEM non-essential amino acids, 1% penicillin/streptomycin, 1% sodium pyruvate and 1% sodium bicarbonate (all 100x, Life Technologies). Cells were passaged once a week using trypsin (0.05%, Life Technologies) and grown in a humidified incubator with 5% CO_2 at 37°C. Cell medium was changed at 24 h and 96 h post-trypsinization.

For uptake experiments, 2×10^5 cells (1 mL) were seeded in 24-well cell culture plates (Nunc) and for confocal microscopy 3×10^5 cells (1 mL) were plated in 35 mm FluoroDish cell culture dishes (WPI). In both case, medium was exchanged after 24 h and cells were used 48 h after seeding. All cells used in experiments were between passages 9 and 25 and were regularly tested for mycoplasma contamination.

2.4. Cellular uptake of TAMRA-labeled peptides

Caco-2 cells were seeded in 24-well cell culture plates and cultured as described above. Afterwards, they were rinsed twice with D-PBS (Life Technologies) and incubated with 500 µL of 1 µM TAMRA-labeled peptides in OptiMEM (Life Technologies) for 1.5 hours at 37°C and 5 % CO_2. The incubation medium was then removed and the cells were rinsed twice with D-PBS. To remove peptides that could have adhered to the extracellular membrane, cells were incubated for 10 min with 100 µL 0.05% trypsin at 37°C, 5% CO_2. Detached cells were transferred in 1.5 mL tubes after addition of 400 µL D-PBS complemented by 5% FBS, followed by centrifugation (10 min, 4°C, 1,500 rpm). Pellets were taken up in 500 µL D-PBS complemented by 0.5% FBS and 0.1% DAPI (Sigma-Aldrich).

2.4.1. Flow cytometry: Half of the resulting cell suspension was transferred to polystyrene round-bottom tubes (Falcon) then analyzed using a LSR Fortessa cytometer from Becton Dickinson (DAPI: λex = 405 nm / λem = 425-475 nm; TAMRA: λex = 561 nm / λem = 605-625 nm). Exclusion of damaged cells was performed by DAPI staining. For each condition 10,000 events were recorded.

2.4.2. Fluorescence spectrometry: The rest of the cell suspension was centrifuged (10 min, 4°C, 1,500 rpm). Subsequently the supernatant was removed and the cells were lysed 1 h in 100 µL RIPA lysis buffer (50 mM Tris (Sigma-Aldrich), 150 mM NaCl (Sigma-Aldrich), 1% (v/v) Triton X-100 (Euromedex), 0.1% (w/v) sodium dodecylsulfate (SDS, Sigma-Aldrich), pH 8.0) complemented with 10% Sigmafast® protease inhibitor (Sigma-Aldrich). Cell lysates were ultimately centrifuged (10 min, 4°C, 13,200 rpm) to obtain the cytosolic fraction of internalized TAMRA-labeled CPP-conjugates for an adequate comparison to the cytosolic fraction measured by flow cytometry. Uptake was determined by measuring TAMRA emission in black 96-well plates on a PolarStar microplate reader (λex = 544 nm / λem = 590 nm) using 50 µL of supernatant. The fluorescence values were normalized to the total protein concentration using a bicinchoninic acid protein assay (Pierce BCA Protein Assay Kit, Thermo Fisher).

2.5. Determination of the correction factor for fluorescence detection from lysis buffer

1   5(6)-carboxytetramethylrhodamine (TAMRA-COOH, Novabiochem) and all TAMRA-labeled peptides
2   used in this study (Table 1) were dissolved in milliQ water at a stock concentration of 500 µM. The
3   concentration of each peptide solutions was controlled by absorbance at 280 nm using a NanoDrop device
4   (Thermo Scientific) to ensure that fluorescence differences are not due to different peptide
5   concentrations. Absorbance of the dye alone was more than 10-fold lower than the labelled peptide
6   solutions as exemplified by the comparison of TAMRA-MPG-iCAL36 [absorbance = 9.290] *versus* TAMRA
7   alone [absorbance = 0.736]. Concentrations of all TAMRA-labelled peptides were overestimated to 10%,
8   however this factor can be negligible, especially since all peptide concentrations were overestimated in a
9   similar extent. Finally, the stock solutions were diluted in milliQ water at a working concentration of 5 µM.
10   Six different conditions were measured in a black ½ area 96-well plate (Greiner) (50 µL/well) for each
11   peptide: Tris or cell lysate alone (= 0 µM peptide), 0.025 µM, 0.05 µM, 0.1 µM and 0.2 µM diluted in either
12   Tris (50 mM Tris, 150 mM NaCl, pH 8) or cell lysate (For more details, see Supplementary Material).
13   The fluorescence intensities were measured at room temperature (λex = 544 nm / λem = 590 nm) using
14   the PolarStar Omega microplate reader (BMG Labtech). Three independent measurements were
15   performed with two technical replicates. The fluorescence values for each condition were averaged and,
16   for each peptide, plotted in fluorescence *versus* peptide concentrations. The slope (in L.mol^{-1}) of the
17   resulting linear regression was determined for the respective peptide at both buffer conditions.
18   In a first approach, the slope of the curve of each peptide in Tris buffer was applied as correction factor
19   for the TAMRA-labeled peptides (**Figure 1D**). In a second approach, the slope of the curve of each peptide
20   in cell lysate was applied as correction factor for the TAMRA-labeled peptides (**Figure 4**).
21
22
23   **2.6. Fluorescence intensities of TAMRA-labeled peptides**
24   *2.6.1. Measurements using different pH:* Different aqueous mixtures of 0.5 M citric acid (Sigma-Aldrich)
25   and 0.5 M monosodium phosphate (Fluka) solutions covering a pH range of 5-8 were prepared to assess
26   the influence of pH on peptide fluorescence. Before diluting the peptide in the buffers with different pH
27   values, actual pH values were checked using a pH-meter (Eutech Instruments).
28   *2.6.2. Measurements using detergents:* Four different buffers were prepared to assess the influence of
29   detergents on peptide fluorescence: 1. 50 mM Tris buffer (pH 8) without detergents, 2. 50 mM Tris buffer
30   (pH 8) containing 1% (v/v) Triton X-100, 3. 50 mM Tris buffer (pH 8) containing 0.1% (w/v) SDS and 4. 50
31   mM Tris buffer containing both detergents (= RIPA buffer).
32   For both measurements, the TAMRA-labeled peptides were diluted to a final concentration of 0.2 µM
33   in the different buffers in a black ½ area 96-well plate (Greiner) (50 µL/well). The fluorescence intensities
34   were then measured at room temperature (λex = 544 nm / λem = 590 nm) using the PolarStar Omega
35   microplate reader (BMG Labtech).
36
37   **2.7. Structure determination by circular dichroism**
38   Circular dichroism spectra of the peptide (80 µM final concentration) were recorded with an optical
39   path of 1 mm on a Jasco 810 (Japan) dichrograph in quartz suprasil cells (Hellma). Peptide signal was first
40   recorded alone in 180 µL milliQ water. After addition of 20 µL of 1% (w/v) SDS (final concentration: 0.1%
41   (w/v)) and homogenization of the solution a second measurement was performed. For each measurement,
42   spectra of 3 accumulations were recorded between 190 and 260 nm (0.5 nm data pitch, 1 nm bandwidth)
43   using the standard sensitivity.
44

2.8. Intracellular localization of TAMRA-labeled peptides

Caco-2 cells were seeded and cultured in FluoroDish cell culture dishes as described above. Cells were rinsed twice with D-PBS (Life Technologies) and incubated with 1000 µL of either 1 µM or 5 µM TAMRA-labeled peptides in OptiMEM (Life Technologies) for 3 hours at 37°C and 5 % CO_2. 10 min before the end of the incubation, 1 µg/mL Hoechst 33342 (Sigma-Aldrich) and 1 µg/mL WGA-Alexa488 (Invitrogen) were added for nuclei and membrane staining, respectively. The incubation medium was then removed, cells were rinsed twice with D-PBS and covered with 1.5 mL of FluoroBrite (Life Technologies). Fluorescence was observed at 37°C with a Leica SP5-SMD confocal microscope (Leica HCX PL Apo CS 63x/1.4NA oil objective lens; Hoechst 33342: λex = 405 nm / λem = 415-485 nm; TAMRA: λex = 561 nm / λem = 571-611 nm; Alexa488: λex = 488 nm / λem = 498-548 nm). Image acquisition was done sequentially to minimize crosstalk between the fluorophores. Each confocal image was merged and adjusted with the same brightness and contrast parameters using the ImageJ software.

2.9. Fluorescence spectra measurements

2.9.1. Self-quenching experiments: Fluorescence spectra of serially diluted solutions of 5(6)-carboxytetramethylrhodamine, *T36 and *W36 in milliQ water (200 µM peptide stock solution) or DMSO (10 mM peptide stock solution) were recorded on a PTI fluorimeter (λex = 553 nm / λem = 565-625 nm, with respective bandwidths of 1 nm and 1.5 nm).

2.9.2. TAMRA-LUV and TAMRA-tryptophan quenching: Serially diluted solutions of LUV reflecting the plasma membrane lipid composition (100 µM stock solution) (for LUV preparation see Supplementary Material) or L-tryptophan (50 mM stock solution) in milliQ water were prepared. 5(6)-carboxytetramethylrhodamine, *T36 or *W36 were added (final peptide concentration of 500 nM) and the fluorescence spectra of the solutions were recorded on a PTI fluorimeter (λex = 553 nm / λem = 565-625 nm, with respective bandwidths of 1 nm and 1.5 nm).

2.10. Liposome leakage assay

Leakage measurements were performed as described elsewhere [28] (see also the Supplementary Material for LUV preparation). Leakage was measured as an increase in fluorescence intensity (λex = 360 nm / λem = 530 nm, with respective bandwidths of 2 nm and 7 nm) upon addition of either iCAL36 or a CPP-iCAL36 (final peptide concentration of 2.5 µM) to 1 mL of LUVs (100 µM) in buffer (20 mM HEPES, 145 mM NaCl, pH 7.4). 100% fluorescence was achieved by solubilizing the membranes with 0.1% (v/v) Triton X-100 resulting in the completely unquenched probe.

2.11. Peptide interaction with the lipids in cell pellets

Caco-2 cells were incubated as described in the section "Cellular uptake of TAMRA-labeled peptides" After cell trypsinization, the cell pellets were taken up in 200 µL 50 mM Tris buffer, pH 8 (composition as described above). 50 µL of the resulting cell suspension was transferred to black ½ area 96-well plates (Greiner), then the rest of the cell suspension was centrifuged (10 min, 4°C, 1,500 rpm) and the cells were lysed as described above. Cell lysates were ultimately centrifuged (10 min, 4°C, 13,200 rpm) and 50 µL of supernatant was transferred to black ½ area 96-well plates. Fluorescence signal was determined by measuring TAMRA emission (λex = 544 nm / λem = 590 nm) on a PolarStar Omega microplate reader (BMG Labtech).

3. RESULTS AND DISCUSSION

3.1. Discrepancies in CPP uptake quantification upon used methods

Flow cytometry is generally used to screen or evaluate the cellular uptake of fluorescently-labeled CPPs or CPP-conjugates in single cells. However, with regard to an internalization in polarized epithelial cells, this method is not suitable due to tight junction formation between the cells prohibiting cell individualization. As this limitation is not encountered when performing quantitative fluorescence spectroscopy on cell lysates, we started to compare quantitatively the internalization of four CPP-conjugates using both flow cytometry and fluorescence spectroscopy on non-confluent Caco-2 cells, in order to assess the compatibility of the results between both methods. As cargo, we selected the peptide iCAL36, a potent therapeutic in the context of cystic fibrosis [19,20] (**Table 1**).

The four TAMRA-labeled (noted with *) CPP-conjugates as well as the *iCAL36 cargo alone (noted *36) were incubated for 1.5 h on Caco-2 cells. After washing steps, the cells were trypsinized to digest the cell surface-bound peptides and to detach cells. Cells were then washed and split in two batches (250 μL each): one for flow cytometry and one to be lyzed for fluorescence spectroscopy measurements. In both cases, only the cytosolic fluorescence intensities of the TAMRA-labeled peptides were assessed because trypsinization and centrifugation steps removed all membrane-bound or membrane-entrapped peptides. To enable a relative comparison of fluorescence intensities measured by both methods, values were normalized by the *iCAL36 value (**Figure 1A and B**). Surprisingly, even after this normalization, the measured values for all CPP-conjugates were highly divergent between both methods.

First, we evaluated potential cytotoxic effects based on the CPP-conjugate incubations by analyzing the DAPI internalization during flow cytometry or by performing a LDH cytotoxicity assay for the fluorescence spectroscopy. In both cases, the viability of the cells incubated with the CPP-conjugates was identical to the one of non-treated cells (**Figure S1A and S1B**), suggesting an absence of cytotoxic effect.

Afterwards, we looked in details to the experimental conditions. For the fluorescence spectroscopy measurements, cells are lysed to have access to the internalized fluorescently labeled peptides. In contrast, during flow cytometry, the fluorescently labeled peptides are surrounded by intact cell content (organelles, proteins, oligonucleotides, lipids etc.) which could have an impact on the dye properties. As this environment could not be reproduced adequately in an assay tube, flow cytometry results should be always compared to other methods such as confocal microscopy.

To identify a possible effect of the peptide sequence on the TAMRA fluorescence intensity, independently of the presence of cell constituents, a comparative fluorescence measurement was performed on the dye alone or coupled to the different peptides in a dose-dependent manner in Tris buffer. **Figure 1C** clearly revealed that the fluorescence intensity differs depending on the analyzed compound. Thus, the slope of each curve could be applied as a corrective factor for the TAMRA-labeled peptides (**Figure 1D**) compared to the dye alone. After this correction, a slightly better coherence between both methods was observed for *iCAL36, *Tat-iCAL36 and *MPG-iCAL36. However, the values for *C6M1-iCAL36 or *WRAP5-iCAL6 were only slightly affected by the correction.

3.2. Factors influencing the fluorescence intensity of TAMRA-labeled CPP-iCAL36 measured from cell lysate

1

2   Quantitative emission of fluorescence dyes can be influenced by different parameters of the used lysis
3   buffer such as pH, salt concentration or the presence of detergents. The surrounding medium can have an
4   impact on the position, shape and intensity of absorption and emission spectra of a dye moiety.
5   We first looked at the consequence of a pH shift. Indeed, fluorescein which is classically used as peptide
6   labeling has important solvatochromic properties, losing nearly totally its signal at the low pH values which
7   can be encountered in acidic cellular compartments [29]. TAMRA-labeled CPP-iCAL36 conjugates (0.2 µM)
8   were consequently diluted in a series of citric acid/sodium monophosphate buffers covering a pH range of
9   5-8 representative of the diversity of cellular compartments, and measured by fluorescence spectroscopy
10 in the absence of cells (**Figure 2A**). In all tested conditions no significant changes of the TAMRA
11 fluorescence were observed for *MPG-iCAL36, *WRAP5-iCAL36 and *C6M1-iCAL36, confirming that this
12 rhodamine dye is not affected by variations in pH values between 5 and 8 which is an important advantage
13 for many biological applications [30]. Curiously, for *Tat-iCAL36 we see an increase in fluorescence (~30%)
14 at more acidic buffer conditions (pH 6 to 5). Compared to fluorescein labeled conjugates, we will obtain in
15 increased signal if the Tat-iCAL36 conjugate will be internalized via an endocytosis dependent pathway.
16   Comparing both used buffers with pH 8, we observed also differences in the measured fluorescence
17 intensity: a 24% increase for *Tat-iCAL36 (103,693 ± 2,848 for Tris *versus* 136,262 ± 4,694 for citric acid)
18 and a 36% decrease for *MPG-iCAL36 (68,132 ± 5,731 for Tris *versus* 43,614 ± 718 for citric acid). This fact
19 cleary revealed that the buffer composition itself could have an effect on the aquired fluorescence values.
20   Further analyses did not show any influence of salt concentration or presence of DAPI on the TAMRA
21 fluorescence (data not shown). We thus quantified the effect of the detergents present in the RIPA lysis
22 buffer (50 mM Tris, 150 mM NaCl, 1% Triton-X100, 0.1% SDS, pH 8.0 = Tris+(Triton/SDS) by comparison to
23 the Tris/NaCl buffer alone (=Tris) or with one of the detergents (= Tris+Triton or Tris+SDS) in the absence
24 of cells (**Figure 2B**). The fluorochrome alone as well as *iCAL36 nearly show identical fluorescence intensity
25 in the four buffer conditions. Curiously a slight reduction (factor 1.5 to 5) could be observed for the dye
26 when it was coupled to the iCAL36 peptide in all buffers.
27   If Triton X-100 is added to the Tris buffer, we observe an increase of the fluorescence intensity
28 compared to the Tris buffer alone especially for *MPG-iCAL36 (6x), *C6M1-iCAL36 (4x) and *WRAP5-
29 iCAL36 (7x). Only *Tat-iCAL36 seems to be unaffected by the addition of Triton X-100. Compared to the
30 Tris buffer alone, the fluorescence intensity of the analyzed peptides increases likewise in the Tris buffer
31 containing SDS (*MPG-iCAL36: 7x, *C6M1-iCAL36: 9x and *WRAP5-iCAL36: 15x), with an even stronger
32 effect of SDS compared to Tris+Triton. Addition of both detergents revealed nearly no additive effect. Only
33 for *MPG-iCAL36, we observe a reduction of fluorescence intensity compared to the (Tris+SDS) or the
34 (Tris+Triton) conditions.
35   Similar effects of detergents on a fluorescence dye were also observed by Illien *et al.* (2016) for the
36 fluorescein-labeled CPP penetratin, especially for Triton-X100 and Nonidet 40 which are closely related
37 detergents [16]. Triton X-100 is non-ionic whereas SDS is an anionic surfactant and therefore, it is
38 reasonable to suppose that they will not have an important interaction with the TAMRA dye which is
39 anionic. However, they could influence the structural behavior of the CPP-iCAL36 conjugates. In particular,
40 SDS can interact with the cationic CPP side chains.
41
42
43 **3.3. Changes in fluorescence intensity by detergents can be due to peptide conformation changes**
44

To evaluate if the detergents can influence the CPP-iCAL36 structure and impact in this way the fluorescence intensity of the corresponding peptide, we performed circular dichroism (CD) measurements. The dichrograms of the four CPP-iCAL36 peptides alone (**Figure 3**, black line) reveal a randomly coiled structure for Tat-iCAL36 and MPG-iCAL36 and a mixed structure for C6M1-iCAL36 and WRAP5-iCAL36. Afterwards, Triton X-100 (1%) and SDS (0.1%) were separately added to the peptide solution. Unfortunately, the Triton X-100 aromatic moiety strongly absorbs in the range of 190 nm - 260 nm, making the evaluation of the peptide structuration impossible in the presence of Triton X-100. In contrast, SDS (0.1%, no SDS micelle formation at this concentration) does not absorb in this range and allows the evaluation of its effects on the peptide structure (**Figure 3**, grey line).

SDS has no significant effect on Tat-iCAL36 conformation and only slight ones on MPG-iCAL36. Those structuration effects are similar to those observed by Deshayes *et al.* (2004) on the MPG peptide with low SDS amount [31]. Additionally, the absence of structuration observed for Tat-iCAL36 mirrors the fact that the Tat peptide does not adopt any specific secondary structure in any condition [32]. However, stronger variations of peptide structure after SDS addition could be observed for C6M1-iCAL36 and WRAP5-iCAL36, resulting in an alpha helical restructuration. Similar results were obtained for C6M1-iCAL36 and WRAP5-iCAL36 in the presence of zwitterionic large unilamellar vesicles (LUVs) at a peptide/lipid molar ratio of 10:1 (**Figure S3**). These visualized conformational changes could hint a disruptive effect of SDS on intramolecular peptide interactions, influencing the position of the fluorescence dye (better accessibility) and resulting in a higher fluorescence signal. It would also imply that all tested peptides do not have the same fluorescence signal in absence of detergents, as probe hindrance could happen.

3.4. A correction factor to normalize discrepancies between cytometry and spectroscopy?

To obtain a more reliable correction factor, we repeated a comparative measurement of the fluorescence intensity of TAMRA dye alone or coupled to the different peptides in a dose-dependent manner, but this time in cell lysate (Caco-2 cells lysate made with RIPA buffer, see Supplementary Material). **Figure 4A** shows significantly different patterns compared to **Figure 1C**. Here, the highest fluorescence intensities are observed for *MPG-iCAL36 and *WRAP5-iCAL36, while for all other TAMRA-labeled peptides an important decrease in fluorescence intensity was revealed.

Interestingly, these signal decreases correlate to peptides with no tryptophan beside those of the iCAL36 sequence (iCAL36 and Tat-iCAL36) or with highest amount of tryptophan residues (C6M1-iCAL36) whereas, the signal increases are observed for the both sequences containing in total 4 aromatic residues (MPG-iCAL36 and WRAP5-iCAL36) (**see Table 1**). The position and the number of aromatic residues seem to play a role on the secondary structure of the peptide and therefore on the brilliance of the TAMRA dye, probably by performing intramolecular π-stacking between the dye and conformationally accessible tryptophan residues.

In conclusion, fluorescence intensity of the *CPP-iCAL36 peptides depends both on the peptide sequence itself and on the presence of detergents such as Triton X-100 and SDS as mentioned above. To take both factors into account, we use the resulting "cell lysate" slope instead of the "Tris" slope as correction factor for each TAMRA-labeled peptide. After the application of the correction factor (**Figure 4B**), we obtain for *Tat-iCAL36 and *MPG-iCAL36 a much-improved coherence of the fluorescence intensity profile between flow cytometry and fluorescence spectroscopy. However, fluorescence signal of *C6M1-iCAL36 and *WRAP5-iCAL36 still seem to be overestimated by fluorescence spectroscopy

detection in comparison to flow cytometry, even when considering the fluorescence variation due to the detergents.

3.5. Visualization of the cellular internalization by confocal microscopy revealed differential localization of the CPP-iCAL36 conjugates

Because both used methods – flow cytometry and fluorescence spectroscopy – displayed different results for *C6M1-iCAL36 and *WRAP5-iCAL36, we used a third commonly used technique to visualize the CPP-conjugate internalization: confocal laser scanning microscopy (CLSM) on living cells. Caco-2 cells were incubated with the corresponding TAMRA-labeled CPP-iCAL36 conjugates using the same incubation time (1.5 h) as used flow cytometry and fluorescence spectroscopy. However, under these conditions, we observed a low signal to noise ratio for all *CPP-iCAL36. To increase the fluorescence signal, the *CPP-iCAL36 concentration could be increased. However, it is known that the CPP concentration to cell ratio could have an impact on their internalization mechanism (endocytosis *versus* direct translocation) resulting in different cellular localization [33].

As control experiment, we have extended the incubation duration of the *CPP-conjugates up to 3 h, resulting in increased fluorescence values measured by flow cytometry (**Figure S2A**): we constated a 2-3 fold increase for *MGP-iCAL36 and *C6M1-iCAL36 and a 4-5 fold enhancement for *WRAP5-iCAL36 and *Tat-iCAL36, respectively, compared to the 1.5 h incubation. However, the overall internalization ratio of the five TAMRA-labelled peptides stayed quite similar. For that reason, we preferred to increase the incubation time up to 3 h in order to obtain higher peptide accumulation within the cell (higher fluorescence signal). After nucleus (Hoechst) and membrane (WGA-Alexa488) labeling, we could observe two different localization patterns of the peptides (**Figure 5**).

First, we performed control experiments without peptide (OptiMEM) or with *iCAL36 to show that no auto-fluorescence nor *iCAL36 (without CPP) internalization are seen, respectively (**Figure 5**). For the four *CPP-iCAL36 conjugates, two different cellular localization patterns are visible. *Tat-iCAL36 and *MPG-iCAL36 are located in a punctuated pattern in the cytoplasm of Caco-2 cells with more fluorescence for *MPG-iCAL36 confirming the results from flow cytometry and fluorescence spectroscopy. On the other hand, *C6M1-iCAL36 and *WRAP5-iCAL36 are mostly stuck at the plasma membrane showing in both cases a co-localization with the membrane labeling of WGA-Alexa488 (orange merged color), indicating a localization of the peptides either bound at or inside the plasma membrane.

Because a trypsinization step is not applicable in the case of CLSM experiments, the observed signal might involve peptide externally bound to the membrane. Furthermore, to our best knowledge the TAMRA dye could not be quenched with trypan blue as it is possible for fluorescein [16,22]. Thus, other methods had to be used to clarify what happened with both peptides at the plasma membrane to explain the divergent results obtained in flow cytometry and fluorescence spectroscopy.

3.6. Self-quenching of TAMRA dye at high peptide concentration

The arrangement of peptides bound to the plasma membrane can be approached by a two-dimensional space in which peptides are locally concentrated, and where peptide–peptide proximity interactions thus become highly prevalent [34]. It is known that rhodamine dyes such as TAMRA are able to perform self-

quenching if they are in direct proximity [35]: in this context, it is likely that TAMRA/TAMRA quenching could take place on the outside of the plasma membrane.

To explore this possibility, we recorded fluorescence spectra of the TAMRA dye alone and the TAMRA-labeled Tat-iCAL36 and WRAP5-iCAL36 peptides as representative examples (**Figure 6A, B and C**). At the lowest concentration of 2 µM, peptide spectra show a fluorescence maximum around ~570 nm for the dye alone and of ~575 nm for the *CPP-iCAL36 peptides. Increasing the concentrations of the dye or the dye-labeled peptides induce a non-linear variation of the fluorescence intensity and a red shift in fluorescence emission indicating a change in the local environment of the TAMRA dye. At the highest concentration of 200 µM this fluorescence shift corresponds to 5 nm (569-574 nm) for the dye alone, to 9 nm (574-583 nm) for *Tat-iCAL36 and to 18 nm (575-593 nm) for *WRAP5-iCAL36.

To visualize the potential quenching phenomenon especially for *WRAP5-iCAL36, we selected the fluorescence intensity maxima and plotted the values *versus* the corresponding peptide concentration (**Figure 6D**). We observe a concentration-dependent increase of the fluorescence signal till the maximal concentration of 200 µM for the dye alone and for *Tat-iCAL36. In contrast to these results, we observe a significant quenching effect with *WRAP5-iCAL36 even reflected by a weak decrease of the fluorescence intensity.

To further confirm these observations, we repeated the experiments with a higher concentration range (10 µM to 10 mM) by diluting the peptides in DMSO (**Figure S4** and **Figure 6E**). We observe a concentration-dependent – while this dependence progressively deviates from linearity – increase of the fluorescence signal till a concentration of 100 µM and thereafter, an important loss of the fluorescence signal for all compounds including the dye alone, revealing the self-quenching potential of the TAMRA dye at high concentrations. A significantly stronger quenching effect is observed with *WRAP5-iCAL36 compared to the TAMRA dye alone or to *Tat-iCAL36, indicating that while quenching of the TAMRA probe can happen for any TAMRA-labeled peptide, quenching efficiency is probably affected by the peptide sequence or secondary structure.

These results show that *CPP-iCAL36 are prone to TAMRA self-quenching when they are locally concentrated. The observed fluorescence decrease is accompanied by a red shift of the wavelength of maximal fluorescence emission, which is characteristic of a Förster resonance energy transfer (FRET) phenomenon [36]. π-stacking interactions between an excited fluorophore and one (or several) ground-state analog(s) lead to self-association of the probes and the formation of an excimer displaying dose-dependent red fluorescence shift [37,38].

At the outer plasma membrane, positively-charged CPPs strongly interact with extracellular membrane-associated anionic constituents (phospholipids, proteoglycans, etc.): the resulting CPP accumulation could facilitate short-range dye/dye interactions, leading to a case of template-directed excimer formation such as exploited by Van Arman and Czarnik [39]. This phenomenon would result in quantitative quenching of the dye-labeled peptide at the outside of plasma membrane, such as reported by Swiecicki *et al.* (2016) [40].

However, TAMRA self-quenching cannot fully explain the discrepancies between flow cytometry and fluorescence spectroscopy for *C6M1-iCAL36 and *WRAP5-iCAL36 as: a) *WRAP5-iCAL36 is partly visible in CLSM and b) for these two methods the externally-sticking peptides are removed from the membrane by trypsinization. Indeed, in a former study, we have shown that cell membrane-bound CPPs could be efficiently removed from the cell membrane independently of their peptide sequence [22]. With a trypsin incubation of 10 min (at 37°C) extracellular proteins and the extracellular matrix were cleaved and the bound CPPs were washed-out at the same time.

3.7. Interaction of the TAMRA-CPP-iCAL36 conjugates with lipid membranes

Both TAMRA-labeled CPP-iCAL36 peptides showing an overestimated fluorescence value during fluorescence spectroscopy measurements even after a 10 min trypsinization step (**Figure 1D** and **Figure 4B**) are conjugated to a secondary amphipathic CPP, and are located at or in the cell membrane as clearly revealed by CLSM (**Figure 5**).

Assuming that during the trypsinization step all extra-cellular proteins are cleaved and washed out from the cell membranes together with externally-sticking *CPP-iCAL36 conjugates, we hypothesized that a fraction of peptide still remains between the lipid bilayers, and that a quenching phenomenon would prevent its detection by flow cytometry. To consolidate this hypothesis, we incubated Caco-2 cells with the TAMRA-labeled peptides for 1.5 h followed by a 10 min trypsinization step. After centrifugation and cell suspension in a Tris buffer, the samples were analyzed by quantitative fluorescence spectroscopy, either directly from intact cell pellets or after the addition of lysis buffer (**Figure 7A**). Fluorescence values of intact cells (without lysis buffer = w/o LB) were only normalized to *iCAL36 whereas lyzed cells (with LB) were corrected with the corresponding correction factors as described above (**Figure 4B**) then normalized to *iCAL36. For the *Tat-iCAL36 and *MPG-iCAL36 peptides, we obtained nearly the same fluorescence intensity for both measured conditions. In contrast, we obtain a 20-fold higher fluorescence signal from the lyzed cell pellet incubated with *C6M1-iCAL36 and *WRAP5-iCAL36 as for the non-treated one. This result seems to highlight a more important liberation of the TAMRA-labeled secondary amphipathic CPP-iCAL36 conjugates out of the lipid bilayer giving rise to a fluorescence recovery event of the TAMRA dye. The strong interaction with lipid bilayers was confirmed by a leakage assay as exemplified for the secondary amphipathic peptide WRAP5-iCAL36 compared to Tat-iCAL36 or iCAL36 alone (**Figure 7B**). Large unilamellar vesicles (LUV) encapsulating a quencher and fluorescence dye (no signal detectable) were incubated with the three peptides during the indicated period. If a peptide is able to transiently destabilize the lipid membrane, the fluorescence dye can escape from the LUVs resulting in an increase in measured fluorescence intensity. This is exactly observed for WRAP5-iCAL36 and C6M1-iCAL36 with an endpoint leakage of 85.6% and 70.4% respectively, reflecting the high efficacy of both CPP-conjugates to interact with lipid membrane models and thus likely with cell membranes.

3.8. Membrane proteins and not membrane lipids are likely involved in TAMRA quenching

The environment of the TAMRA-labeled peptides could be influenced by the cell membrane lipids, which could induce potential quenching of the dye when it is inserted in the bilayer. When cells are lysed for fluorescence spectroscopy measurements, the TAMRA-labeled peptides would be released from the bilayer, resulting in a now detectable fluorescence. To give some evidence concerning this hypothesis, we incubated the TAMRA dye alone, *Tat-iCAL36 and *WRAP5-iCAL36 with increasing equivalents of LUVs mimicking the lipid composition of cell membranes (**Figure 8A-C**). For the first two conditions, we observe nearly no changes in the fluorescence intensity maxima. Using the *WRAP5-iCAL36 peptide, we could not measure the expected lipid-based quenching of the TAMRA dye, while a slight increase (1.5-fold) of the fluorescence values was revealed after lipid addition. This agrees with the previous results showing a conformational change of WRAP5-iCAL36 in the presence of SDS or LUV: it is likely that both could disrupt

*WRAP5-iCAL36 intramolecular interactions, and especially intramolecular TAMRA/tryptophan interactions, and provoke a TAMRA fluorescence recovery (**Figure 3**). These results invalided our initial hypothesis that *CPP-iCAL36 fluorescence will be quenched through contacts with membrane lipids. However, quenching can still occur in (not because of) the lipid vesicles, thanks to increased local concentrations of the peptides (self-quenching) which is not assessable with the used method because of the high external peptide concentration.

However, besides its lipid content the cell membrane is composed of various transmembrane (TM) proteins which are particularly enriched in tryptophan residues [41,42]. The versatile molecular properties of those residues play an important role in membrane protein folding and stability: tryptophan has the largest nonpolar surface area, is the most polarizable residue, possesses an indole N-H moiety that is capable of hydrogen bond donation, and displays the greatest electrostatic potential for cation-π interactions [43]. However, beside these important roles, it has been shown that the fluorescence intensity of some fluorescence dyes such as fluorescein or TAMRA is substantially quenched by the proximity of tryptophan residues [44]: this property has notably been applied to the development of "quenchbodies", antibodies involving an intramolecular TAMRA/tryptophan quenching which is abolished upon presentation of its antigen [45]. A hypothesis would be that fluorescence quenching happens inside the lipid bilayer at the contact of TM proteins, hence explaining why quenching could be observed for *C6M1-iCAL36 and *WRAP-iCAL36 (membrane-inserting peptides) and not for *Tat-iCAL36 and *MPG-iCAL36 (no membrane insertion). To highlight the potential effect of membrane tryptophan on *CPP-iCAL36 fluorescence, we titrated the TAMRA dye as well as *Tat-iCAL36 and *WRAP5-iCAL36 with increasing concentrations of tryptophan as a simple model for tryptophan-rich TM proteins (**Figure 8D-F**). For the TAMRA dye and the *Tat-iCAL36 peptide, we could observe a dose-dependent decrease of the fluorescence intensity with 4-fold lower values at the highest tryptophan concentration (50 mM) compared to the starting condition without tryptophan. Curiously, we detect another pattern for the *WRAP5-iCALP36 peptide in the presence of increasing tryptophan concentration: first the fluorescence intensity increases with 0.5 mM tryptophan to a 1.4-fold higher value, then a successive scale-down is visible, reaching a 2.8 lower value at 50 mM tryptophan compared to the peptide alone. Here, we are probably observing two connected events corresponding to a peptide structuration resulting in better accessibility of the dye (↑ fluorescence) and to TAMRA/tryptophan quenching (↓ fluorescence). Interestingly, no red shift of the fluorescence maximum is observed, further confirming that the quenching mechanism differs from TAMRA self-quenching and would not be based on peptide proximity inside the lipid bilayer.

We are aware that this experimental model used high tryptophan concentrations which are probably not physically present in transmembrane proteins located at the cell membrane. An accurate tryptophan quantification in transmembrane area will be difficult, but it is known from the literature that an unusual abundance of tryptophan in transmembrane proteins exists (3.3% compared with 1.2% of soluble proteins [41]), and that those tryptophans are clustered at the membrane-water interfacial regions of the transmembrane domains of the proteins [46]. Furthermore, it is also known that the amounts and families of proteins in a membrane are highly variable, but tend to correspond to 50% of the mass of a typical plasma membrane [47]. Assuming all these facts, the probability of encountering a tryptophan motif anywhere in the transmembrane area is important. In conclusion, these facts and our results let us hypothesize that TAMRA-labelled peptides trapped in the membrane (such as WRAP5-iCAL36 or C6M1-iCAL36) (**Figure 5**), could undergo TAMRA/tryptophan quenching induced by the high probability that a TAMRA unit located at the cell membrane is closed to at least one tryptophan of a transmembrane protein.

4. CONCLUSION

In the present work, we have highlighted that significantly diverging results can be obtained with different fluorescence techniques during intracellular uptake quantification of rhodamine-labeled CPP-conjugates (see **Figure 9**). In particular, tryptophan-rich CPPs can undergo both intramolecular and intermolecular dye/tryptophan interactions, consequently influencing the fluorescence intensity of the labeled peptide and biasing in the estimation of the cellular uptake.

First, within the peptide sequence, intramolecular interactions and dye/tryptophan π-stacking can affect peptide structuration and dye environment, resulting in a fluorescence quenching in Tris buffer. However, this quenching is abolished in cell lysate (RIPA lysis buffer) based on the presence of detergents, which can denaturate the peptides forcing them into a more extended/linear state separating the dye from the tryptophan residues (no more quenching). However, for WRAP5-iCAL36 and C6M1-iCAL36, we observed the opposite. The addition of SDS leads to peptide folding in a helical conformation thus preventing dye/tryptophan intramolecular interactions and enhancing peptide fluorescence. In this sense, the detergent content of lysis buffers can induce overestimated fluorescence spectroscopy values. To circumvent this bias, we reported the use of standard fluorescence curves, allowing to compare the intrinsic fluorescence of TAMRA-labeled peptide either with or without detergents and to use the resulting coefficients for value normalization.

The analysis of the cellular localization of TAMRA-CPP-iCAL36 peptides by CLSM first raised surprising concerns, as peptide signal could only be observed in the membrane region for *C6M1-iCAL36 and *WRAP5-iCAL36 and not for *Tat-iCAL36 and *MPG-iCAL36, while all positively-charged peptides are known to strongly interact with the external membrane proteins. We subsequently explained this result by proving that TAMRA-labeled CPP-conjugates undergo dye self-quenching and red shift of their fluorescence spectra when they are locally concentrated, such as at the outer cell surface where their tethering by the negatively-charged external membrane content increase their likeliness of interaction.

Finally, we demonstrated that dye-labeled CPP-conjugates that are capable of membrane insertion (typically, secondary amphipathic peptides) can be sequestered in the cell membrane as shown for C6M1-iCAL36 and WRAP5-iCAL36. In this case, the TAMRA labeled peptide could interact with membrane lipids or tryptophan-rich transmembrane proteins. At this point, it is difficult to give a conclusion about what happens with the fluorophore during membrane sequestration. However, we hypothesize that TAMRA interaction with the tryptophan content of membrane proteins may result in a *CPP-iCAL36 fluorescence quenching. This quenching is abolished after membrane solubilization by detergents, and lead to an overestimation of the measured fluorescence which accounts for both cytosolic and intramembrane-trapped peptide.

All these results emphasize the need of careful multi-method analysis of CPP uptake, especially when detergents-based buffers are involved. As CLSM does not allow the visualization of intramembrane-trapped CPP fraction, the uptake of amphipathic CPPs presenting lipid membrane interaction should always be compared by several fluorescence-based methods (fluorescence spectroscopy, flow cytometry and CLSM) to avoid an overestimation of the cellular internalization.

14
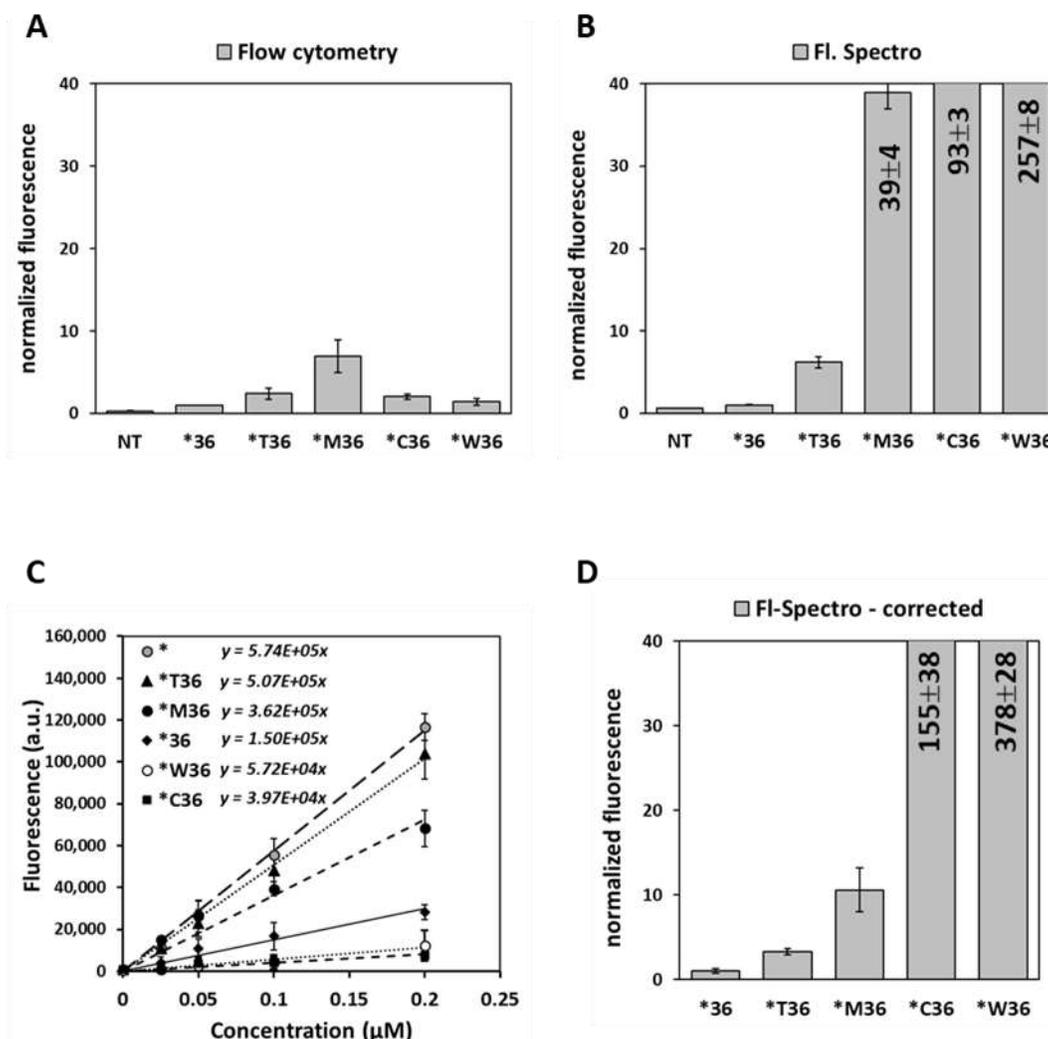
3
4 **Figure 1: Comparison of the internalization of TAMRA-labeled CPP-iCAL36 conjugates measured by flow**
5 **cytometry or by fluorescence spectroscopy after cell lysis.**
6 Caco-2 cells were incubated with 1 µM TAMRA-labeled peptide solution in OptiMEM for 1.5 h. After cell
7 trypsinization (to remove external peptide) each cell suspension was split in two batches (250 µL each).
8 One pool was analyzed by flow cytometry (**A**) and the other was lyzed and transfer in a microtiter plate for
9 an acquisition by fluorescence spectroscopy (**B**). All fluorescence values were normalized to *iCAL36 (= 1).
10 (**C**) Dose-dependent fluorescence measurement of TAMRA alone, TAMRA-iCAL36 and of the four TAMRA-
11 CPP-iCAL36 conjugates (0.025 µM, 0.05 µM; 0.1 µM and 0.2 µM) in Tris buffer to obtain a slope as
12 correction factor.
13 (**D**) Fluorescence values of the internalized peptide were corrected by the slope previously determined.
14 All graphs represent the mean $\pm$ SD from n $\geq$ 3 independent experiments measured in duplicates.
15 * indicates TAMRA alone or TAMRA-labeling of the peptide. 36 = iCAL36, T36 = Tat-iCAL36, M36 = MPG-
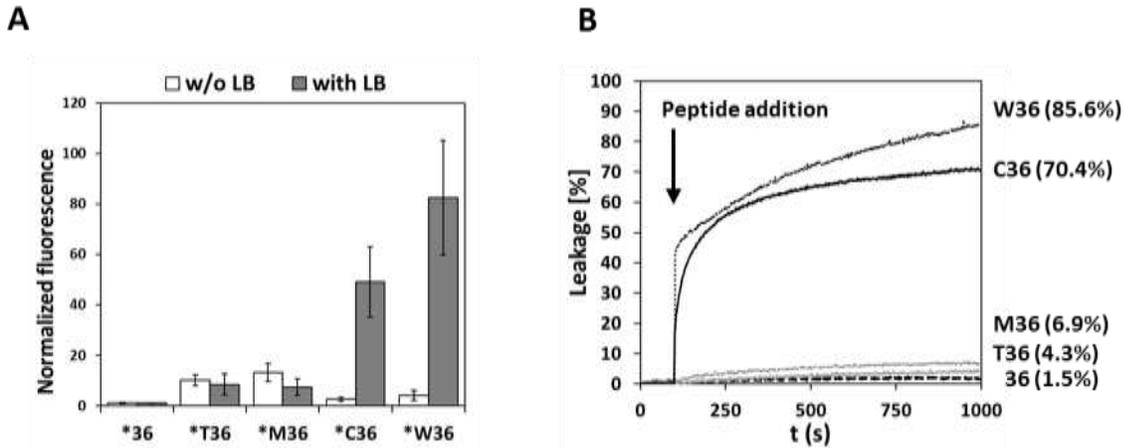16 iCAL36, C36 = C6M1-iCAL36 and W36 = WRAP5-iCAL36.
17

1
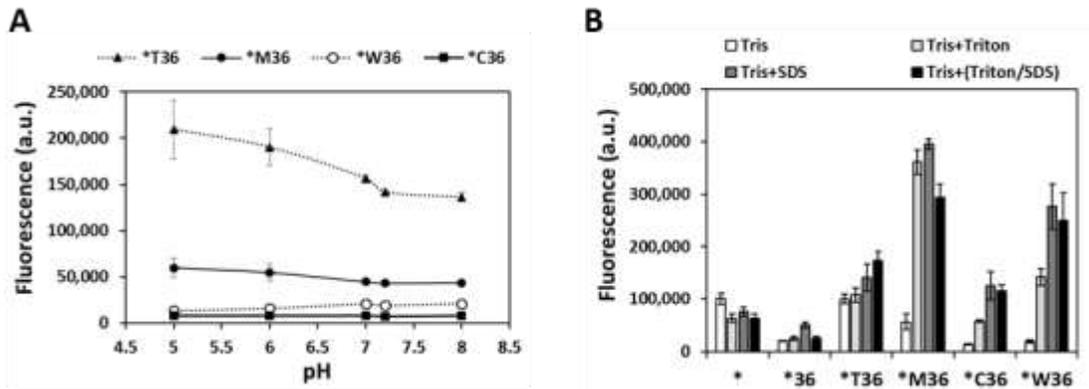
2 **Figure 2: Evaluation of the conditions influencing the fluorescence intensities of the TAMRA-labeled**
3 **CPP-iCAL36 conjugates.**
4 (**A**) Evaluation of the pH dependence of the TAMRA-labeled CPP-conjugates (0.2 µM) using a citric
5 acid/sodium monophosphate buffer covering a pH range of 5-8 measured by fluorescence spectroscopy.
6 (**B**) Evaluation of the effect of detergents on the fluorescence intensity of TAMRA-labeled CPP-conjugates
7 (0.2 µM) measured by fluorescence spectroscopy.
8 Both graphs represent the mean ± SD from n ≥ 3 independent experiments measured in duplicates. *
9 indicates the TAMRA alone or the peptide labeling. 36 = iCAL36, T36 = Tat-iCAL36, M36 = MPG-iCAL36, C36
10 = C6M1-iCAL36 and W36 = WRAP5-iCAL36.

11
12
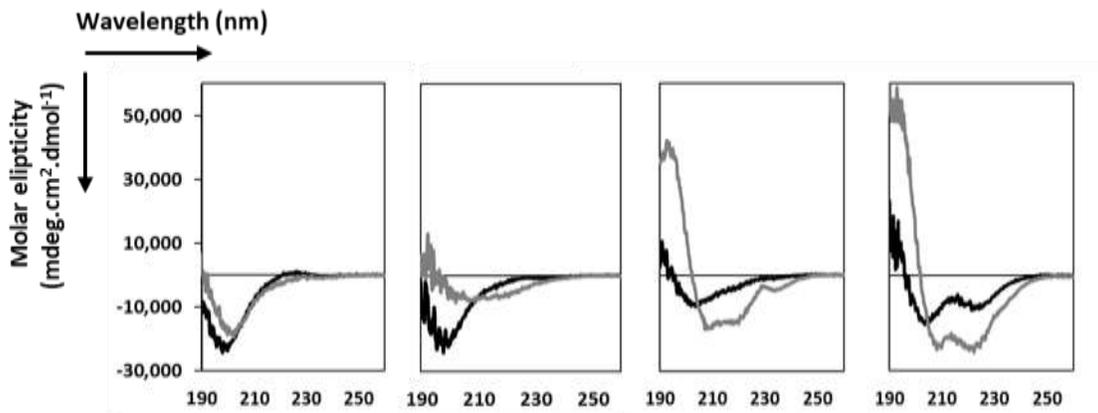
Peptide	T36	M36	C36	W36
- SDS (black line)	coiled (+++)	coiled (+++)	α-helix (+/-), coiled (++)	α-helix (+), β-turn (+) or coiled (+)
+ SDS (grey line)	coiled (+++)	α-helix (+), coiled (++)	α-helix (++), coiled (+)	α-helix (+++)

13
14 **Figure 3. Characterization of the CPP-iCAL36 conformational changes in the presence of SDS.**
15 Far-UV CD spectra of Tat-iCAL36, MPG-iCAL36, C6M1-iCAL36 and WRAP5-iCAL36 were measured in the
16 absence (black line) or in the presence of 0.1% SDS (grey line). Relative proportion of typical structures
17 were estimated qualitatively.

18
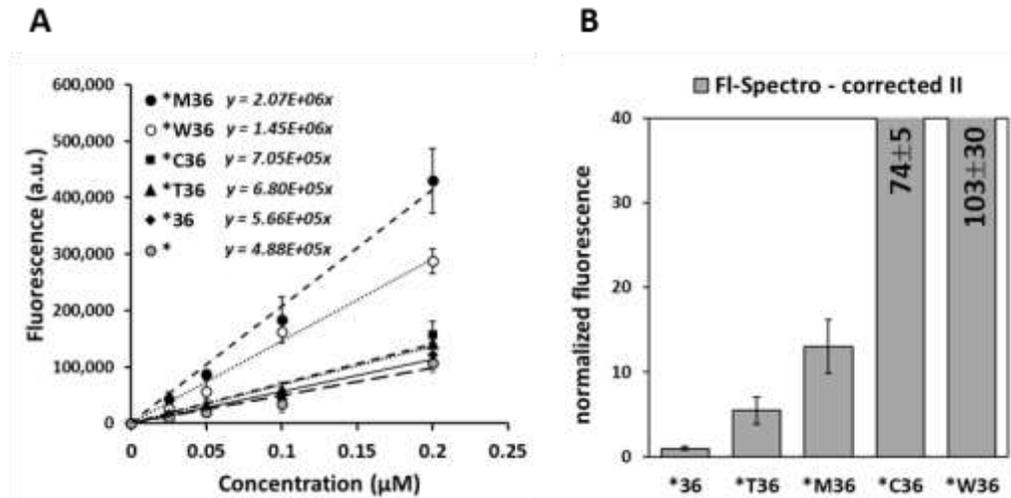
Figure 4. Determination of the correction factor to evaluate results from fluorescence spectroscopy.

(**A**) Dose-dependent fluorescence measurement of TAMRA alone, *iCAL36 and of the four *CPP-iCAL36 conjugates (0.025 µM, 0.05 µM; 0.1 µM and 0.2 µM) in Caco-2 cell lysate of RIPA buffer to obtain a slope as correction factor.

(**B**) Fluorescence values of the internalized peptide were corrected by the correction factor (slope of Figure 4A).

All graphs represent the mean $\pm$ SD from n $\geq$ 3 independent experiments measured in duplicates.

* indicates TAMRA alone or TAMRA-labeling of the peptide. 36 = iCAL36, T36 = Tat-iCAL36, M36 = MPG-iCAL36, C36 = C6M1-iCAL36 and W36 = WRAP5-iCAL36.

Figure 5. Cellular localization of the TAMRA-labeled CPP-iCAL36 conjugates.
Living Caco-2 cells were visualized by CLSM after 3 h incubation with the *CPP-iCAL36 conjugates (Red) in OptiMEM. 10 min before the end of the incubation, Hoechst dye (Blue) and WGA-Alexa488 (Green) were added. Cells were washed and covered with FluoroBrite before imaging. White bars represent 20 µm. 36 = iCAL36, T36 = Tat-iCAL36, M36 = MPG-iCAL36, C36 = C6M1-iCAL36 and W36 = WRAP5-iCAL36. * indicates TAMRA-labeling of the peptide
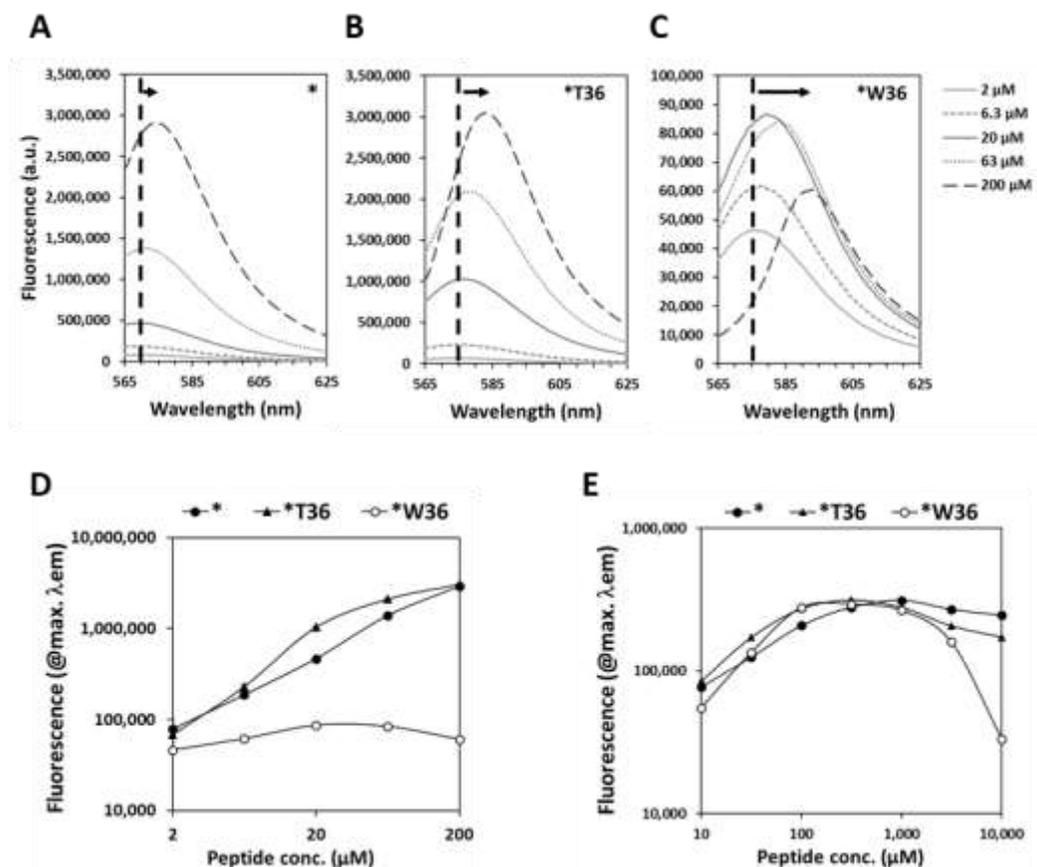
Figure 6. Evaluation of the TAMRA dye properties depending on the peptide concentration.
Representative fluorescence spectra of TAMRA alone (**A**), TAMRA labeled Tat-iCAL36 (**B**) and WRAP5-iCAL36 (**C**) measured in a dose-dependent manner (2 µM to 200 µM diluted in H_2O). When the fluorescence values of the maximal emission wavelength are plotted *versus* the peptide concentration (**D**), the fluorescence signal increase in a nearly linear dose-dependent manner for TAMRA and *Tat-iCAL36 till the highest concentration whereas the signal started to decrease at 63 µM for *WRAP5-iCAL36.
(**E**) Same experiments were repeated with both CPP-peptides diluted in DMSO to obtain higher concentrations (from 10 µM to 10 mM) (See also **Figure S1**). In this case, the fluorescence signal increase in a non-linear manner till a concentration of 100 µM and decrease significantly afterwards, underlining strong quenching of the TAMRA dye.
Graphs (A, B and C) represent the mean of 2 independent experiments. * indicates the TAMRA alone or TAMRA-peptide labeling. 36 = iCAL36, T36 = Tat-iCAL36 and W36 = WRAP5-iCAL36. Dotted lines correspond to the fluorescence emission at the highest wavelength (max λem) for each compound at 10 µM and the arrow showed the red shift.

19

Figure 7: Evaluation of the membrane interaction of the TAMRA-labeled CPP-iCAL36 conjugates.

(**A**) Analysis of the TAMRA dye alone as well as the indicated TAMRA-labeled peptide at the cellular membrane. Caco-2 cells were incubated with the different compounds for 1.5 h following by a trypsinization step (10 min). Fluorescence intensities of the intact (w/o LB) and lyzed (with LB) cell pellets were measured by fluorescence spectroscopy.

* indicates TAMRA-peptide labeling. 36 = iCAL36, T36 = Tat-iCAL36, M36 = MPG-iCAL36, C36 = C6M1-iCAL36 and W36 = WRAP5-iCAL36. LB corresponds to "lysis buffer".

(**B**) Comparison of the leakage properties of iCAL36, Tat-iCAL36, MPG-iCAL36, C6M1-iCAL36 and WRAP5-iCAL36 on LUVs [DOPC/SM/Chol (2:2:1)] encapsulating a quencher and a fluorescence dye. Peptides were injected at 100 s and the Triton (positive control = 100% leakage) at 1000 s (n ≥ 2).
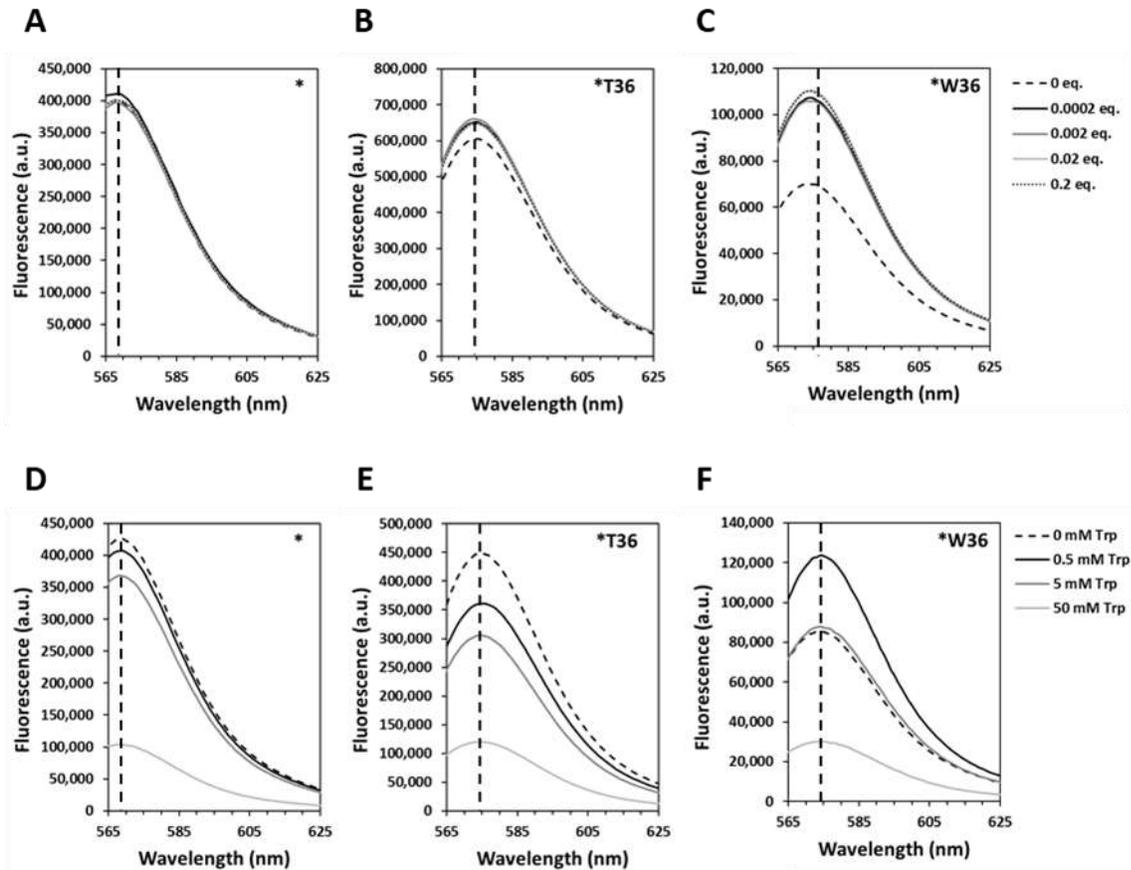
Figure 8. Effect of the addition of phospholipid vesicles or tryptophan on the fluorescence of the TAMRA residue.

(**A - C**) 0.5 µM TAMRA or *CPP-iCAL36 were titrated by increasing LUV [DOPC/SM/Chol (2:2:1)] molar equivalents (0.0002 eq. - 0.02 eq.).

(**D - E**) 0.5 µM TAMRA or *CPP-iCAL36 were titrated by increasing tryptophan concentrations (0.5 mM - 50 mM).

In all conditions, TAMRA fluorescence was excited at 553 nm and the emission spectrum was recorded between 565 nm and 625 nm. Graphs represent the mean of n ≥ 2 independent experiments.
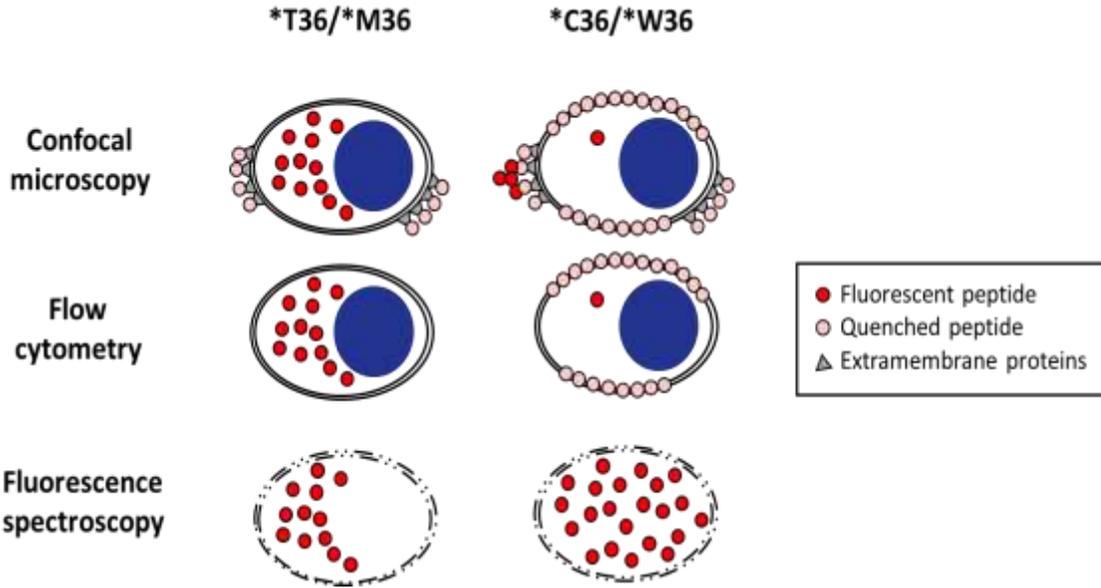
Figure 9. Summarizing model reflecting the discrepancies observed between CLSM, flow cytometry and fluorescence spectroscopy for the uptake of *CPP-iCAL36.

In confocal microscopy, both cytosolic and, if present, self-associated external peptide are visible. In flow cytometry, only cytosolic signal is quantified. In fluorescence spectroscopy, cytosolic signal and, if present, membrane-inserted peptide is quantified.

REFERENCES

[1]   J. Pae, M. Pooga, Peptide-mediated delivery: an overview of pathways for efficient internalization, Ther. Deliv. 5 (2014) 1203–1222. doi:10.4155/tde.14.72.

[2]   K. Cleal, L. He, P.D. Watson, A.T. Jones, Endocytosis, intracellular traffic and fate of cell penetrating peptide based conjugates and nanoparticles, Curr. Pharm. Des. 19 (2013) 2878–2894.

[3]   L.N. Patel, J.L. Zaro, W.-C. Shen, Cell penetrating peptides: intracellular pathways and pharmaceutical perspectives, Pharm. Res. 24 (2007) 1977–1992. doi:10.1007/s11095-007-9303-7.

[4]   D. Derossi, A.H. Joliot, G. Chassaing, A. Prochiantz, The third helix of the Antennapedia homeodomain translocates through biological membranes, J. Biol. Chem. 269 (1994) 10444–10450.

[5]   M. Green, P.M. Loewenstein, Autonomous functional domains of chemically synthesized human immunodeficiency virus tat trans-activator protein, Cell. 55 (1988) 1179–1188.

[6]   A.D. Frankel, C.O. Pabo, Cellular uptake of the tat protein from human immunodeficiency virus, Cell. 55 (1988) 1189–1193.

[7]   A.T. Jones, E.J. Sayers, Cell entry of cell penetrating peptides: tales of tails wagging dogs, J. Control. Release Off. J. Control. Release Soc. 161 (2012) 582–591. doi:10.1016/j.jconrel.2012.04.003.

[8]   W.B. Kauffman, T. Fuselier, J. He, W.C. Wimley, Mechanism Matters: A Taxonomy of Cell Penetrating Peptides, Trends Biochem. Sci. 40 (2015) 749–764. doi:10.1016/j.tibs.2015.10.004.

[9]   G. Guidotti, L. Brambilla, D. Rossi, Cell-Penetrating Peptides: From Basic Research to Clinics, Trends Pharmacol. Sci. 38 (2017) 406–424. doi:10.1016/j.tips.2017.01.003.

[10]   F. Milletti, Cell-penetrating peptides: classes, origin, and current landscape, Drug Discov. Today. 17 (2012) 850–860. doi:10.1016/j.drudis.2012.03.002.

1 [11] J.D. Ramsey, N.H. Flynn, Cell-penetrating peptides transport therapeutics into cells, Pharmacol.
2   Ther. 154 (2015) 78–86. doi:10.1016/j.pharmthera.2015.07.003.
3 [12] A.D. Woldetsadik, M.C. Vogel, W.M. Rabeh, M. Magzoub, Hexokinase II-derived cell-penetrating
4   peptide targets mitochondria and triggers apoptosis in cancer cells, FASEB J. Off. Publ. Fed. Am.
5   Soc. Exp. Biol. 31 (2017) 2168–2184. doi:10.1096/fj.201601173R.
6 [13] M. Gomarasca, T.F.C. Martins, L. Greune, P.R. Hardwidge, M.A. Schmidt, C. Rüter, Bacterial-derived
7   cell-penetrating peptides deliver gentamicin to kill intracellular pathogens, Antimicrob. Agents
8   Chemother. (2017) AAC.02545–16. doi:10.1128/AAC.02545-16.
9 [14] J.P. Richard, K. Melikov, E. Vives, C. Ramos, B. Verbeure, M.J. Gait, L.V. Chernomordik, B. Lebleu,
10   Cell-penetrating peptides. A reevaluation of the mechanism of cellular uptake, J. Biol. Chem. 278
11   (2003) 585–590. doi:10.1074/jbc.M209548200.
12 [15] F. Burlina, S. Sagan, G. Bolbach, G. Chassaing, Quantification of the Cellular Uptake of Cell-
13   Penetrating Peptides by MALDI-TOF Mass Spectrometry, Angew. Chem. Int. Ed. 44 (2005) 4244–
14   4247. doi:10.1002/anie.200500477.
15 [16] F. Illien, N. Rodriguez, M. Amoura, A. Joliot, M. Pallerla, S. Cribier, F. Burlina, S. Sagan, Quantitative
16   fluorescence spectroscopy and flow cytometry analyses of cell-penetrating peptides internalization
17   pathways: optimization, pitfalls, comparison with mass spectrometry quantification, Sci. Rep. 6
18   (2016) 36938. doi:10.1038/srep36938.
19 [17] D. Birch, M.V. Christensen, D. Staerk, H. Franzyk, H.M. Nielsen, Fluorophore labeling of a cell-
20   penetrating peptide induces differential effects on its cellular distribution and affects cell viability,
21   Biochim. Biophys. Acta. 1859 (2017) 2483–2494. doi:10.1016/j.bbamem.2017.09.015.
22 [18] S.F. Hedegaard, M.S. Derbas, T.K. Lind, M.R. Kasimova, M.V. Christensen, M.H. Michaelsen, R.A.
23   Campbell, L. Jorgensen, H. Franzyk, M. Cárdenas, H.M. Nielsen, Fluorophore labeling of a cell-
24   penetrating peptide significantly alters the mode and degree of biomembrane interaction, Sci. Rep.
25   8 (2018) 6327. doi:10.1038/s41598-018-24154-z.
26 [19] L. Vouilleme, P.R. Cushing, R. Volkmer, D.R. Madden, P. Boisguerin, Engineering peptide inhibitors
27   to overcome PDZ binding promiscuity, Angew. Chem. Int. Ed Engl. 49 (2010) 9912–9916.
28   doi:10.1002/anie.201005575.
29 [20] P.R. Cushing, L. Vouilleme, M. Pellegrini, P. Boisguerin, D.R. Madden, A stabilizing influence: CAL
30   PDZ inhibition extends the half-life of ΔF508-CFTR, Angew. Chem. Int. Ed Engl. 49 (2010) 9907–
31   9911. doi:10.1002/anie.201005585.
32 [21] E. Vivès, P. Brodin, B. Lebleu, A truncated HIV-1 Tat protein basic domain rapidly translocates
33   through the plasma membrane and accumulates in the cell nucleus, J. Biol. Chem. 272 (1997)
34   16010–16017.
35 [22] J. Mueller, I. Kretzschmar, R. Volkmer, P. Boisguerin, Comparison of cellular uptake using 22 CPPs in
36   4 different cell lines, Bioconjug. Chem. 19 (2008) 2363–2374. doi:10.1021/bc800194e.
37 [23] J. Müller, J. Triebus, I. Kretzschmar, R. Volkmer, P. Boisguerin, The agony of choice: how to find a
38   suitable CPP for cargo delivery, J. Pept. Sci. Off. Publ. Eur. Pept. Soc. 18 (2012) 293–301.
39   doi:10.1002/psc.2396.
40 [24] M. Jafari, W. Xu, S. Naahidi, B. Chen, P. Chen, A new amphipathic, amino-acid-pairing (AAP) peptide
41   as siRNA delivery carrier: physicochemical characterization and in vitro uptake, J. Phys. Chem. B.
42   116 (2012) 13183–13191. doi:10.1021/jp3072553.
43 [25] K. Konate, M. Dussot, G. Aldrian, A. Vaissière, V. Viguier, I.F. Neira, F. Couillaud, E. Vivès, P.
44   Boisguerin, S. Deshayes, Peptide-Based Nanoparticles to Rapidly and Efficiently "Wrap "n Roll"
45   siRNA into Cells," Bioconjug. Chem. 30 (2019) 592–603. doi:10.1021/acs.bioconjchem.8b00776.
46 [26] G.T. Dempsey, J.C. Vaughan, K.H. Chen, M. Bates, X. Zhuang, Evaluation of fluorophores for optimal
47   performance in localization-based super-resolution imaging, Nat. Methods. 8 (2011) 1027–1036.
48   doi:10.1038/nmeth.1768.

[27] N.O. Mchedlov-Petrossyan, V.V. Ivanov, Effect of the solvent on the absorption spectra and protonation of fluorescein dye anions, Russ. J. Phys. Chem. 81 (2007) 112–115. doi:10.1134/S0036024407010219.

[28] A. Vaissière, G. Aldrian, K. Konate, M.F. Lindberg, C. Jourdan, A. Telmar, Q. Seisel, F. Fernandez, V. Viguier, C. Genevois, F. Couillaud, P. Boisguerin, S. Deshayes, A retro-inverso cell-penetrating peptide for siRNA delivery, J. Nanobiotechnology. 15 (2017) 34. doi:10.1186/s12951-017-0269-2.

[29] M.J. Doughty, pH dependent spectral properties of sodium fluorescein ophthalmic solutions revisited, Ophthalmic Physiol. Opt. 30 (2010) 167–174. doi:10.1111/j.1475-1313.2009.00703.x.

[30] M. Longmire, M. Ogawa, Y. Hama, N. Kosaka, C.A.S. Regino, P.L. Choyke, H. Kobayashi, Determination of Optimal Rhodamine Flurophore for In Vivo Optical Imaging, Bioconjug. Chem. 19 (2008) 1735–1742. doi:10.1021/bc800140c.

[31] S. Deshayes, S. Gerbal-Chaloin, M.C. Morris, G. Aldrian-Herrada, P. Charnet, G. Divita, F. Heitz, On the mechanism of non-endosomial peptide-mediated cellular delivery of nucleic acids, Biochim. Biophys. Acta BBA - Biomembr. 1667 (2004) 141–147. doi:10.1016/j.bbamem.2004.09.010.

[32] E. Eiríksdóttir, K. Konate, Ü. Langel, G. Divita, S. Deshayes, Secondary structure of cell-penetrating peptides controls membrane interaction and insertion, Biochim. Biophys. Acta BBA - Biomembr. 1798 (2010) 1119–1128. doi:10.1016/j.bbamem.2010.03.005.

[33] F. Duchardt, M. Fotin-Mleczek, H. Schwarz, R. Fischer, R. Brock, A Comprehensive Model for the Cellular Uptake of Cationic Cell-penetrating Peptides, Traffic. 8 (2007) 848–866. doi:10.1111/j.1600-0854.2007.00572.x.

[34] C. Aisenbrey, B. Bechinger, Molecular Packing of Amphipathic Peptides on the Surface of Lipid Membranes, Langmuir. 30 (2014) 10374–10383. doi:10.1021/la500998g.

[35] A. Shiba, E. Kinoshita-Kikuta, E. Kinoshita, T. Koike, TAMRA/TAMRA Fluorescence Quenching Systems for the Activity Assay of Alkaline Phosphatase, Sensors. 17 (2017). doi:10.3390/s17081877.

[36] Y.H. Park, Y. Kim, H. Sohn, K.-S. An, Concentration quenching effect of organic light-emitting devices using DCM1-doped tetraphenylgermole, J. Phys. Org. Chem. 25 (2012) 207–210. doi:10.1002/poc.1893.

[37] J.R. Lakowicz, Principles of Fluorescence Spectroscopy, 3rd ed., Springer US, 2006. //www.springer.com/gp/book/9780387312781.

[38] W. Wang, J.J. Han, L.-Q. Wang, L.-S. Li, W.J. Shaw, A.D.Q. Li, Dynamic π–π Stacked Molecular Assemblies Emit from Green to Red Colors, Nano Lett. 3 (2003) 455–458. doi:10.1021/nl025976j.

[39] S.A. Van Arman, A.W. Czarnik, A general fluorescence assay for enzyme catalyzed polyanion hydrolysis based on template directed excimer formation. Application to heparin and polyglutamate, J. Am. Chem. Soc. 112 (1990) 5376–5377. doi:10.1021/ja00169a070.

[40] J.-M. Swiecicki, F. Thiebaut, M. Di Pisa, S. Gourdin -Bertin, J. Tailhades, C. Mansuy, F. Burlina, S. Chwetzoff, G. Trugnan, G. Chassaing, S. Lavielle, How to unveil self-quenched fluorophores and subsequently map the subcellular distribution of exogenous peptides, Sci. Rep. 6 (2016) 20237. doi:10.1038/srep20237.

[41] M. Schiffer, C.H. Chang, F.J. Stevens, The functions of tryptophan residues in membrane proteins, Protein Eng. 5 (1992) 213–214.

[42] K.M. Sanchez, G. Kang, B. Wu, J.E. Kim, Tryptophan-lipid interactions in membrane protein folding probed by ultraviolet resonance Raman and fluorescence spectroscopy, Biophys. J. 100 (2011) 2121–2130. doi:10.1016/j.bpj.2011.03.018.

[43] J.P. Gallivan, D.A. Dougherty, Cation-pi interactions in structural biology, Proc. Natl. Acad. Sci. U. S. A. 96 (1999) 9459–9464.

[44] N. Marmé, J.-P. Knemeyer, M. Sauer, J. Wolfrum, Inter- and intramolecular fluorescence quenching of organic dyes by tryptophan, Bioconjug. Chem. 14 (2003) 1133–1139. doi:10.1021/bc0341324.

[45] R. Abe, H. Ohashi, I. Iijima, M. Ihara, H. Takagi, T. Hohsaka, H. Ueda, "Quenchbodies": quench-based antibody probes that show antigen-dependent fluorescence, J. Am. Chem. Soc. 133 (2011) 17386–17394. doi:10.1021/ja205925j.

[46] H. Sun, D.V. Greathouse, O.S. Andersen, R.E. Koeppe, The preference of tryptophan for membrane interfaces: insights from N-methylation of tryptophans in gramicidin channels, J. Biol. Chem. 283 (2008) 22233–22243. doi:10.1074/jbc.M802074200.

[47] B. Alberts, A. Johnson, J. Lewis, M. Raff, K. Roberts, P. Walter, Membrane Proteins, Mol. Biol. Cell 4th Ed. (2002). https://www.ncbi.nlm.nih.gov/books/NBK26878/ (accessed June 5, 2019).

ACKNOWLEDGEMENTS

1 **SUPPLEMENTAL MATERIALS AND METHODS:**

2

3 **Peptide synthesis:**

4   Peptide synthesis was performed by LibertyBlue™ Microwave Peptide Synthesizer (CEM Corporation),

5 an additional module of Discover™ (CEM Corporation) combining microwave energy at 2450 MHz to the

6 fluorenylmethoxycarbonyl (Fmoc)/*tert*-butyl (*t*Bu) strategy. If not otherwise mentioned, all chemicals

7 were purchased by Sigma-Aldrich or Carlo Erba.

8   Syntheses were conducted on a 0.25 mmol scale on a Fmoc-Ile-Wang resin (Bachem). Deprotections

9 were performed with 20% piperidine in DMF. All coupling reactions were performed with 5 eq. of DIC in

10 DMF (0.5 M), 5 eq. of Fmoc-protected amino acids in DMF (0.2 M) and 5 eq. of Oxyma in DMF (1 M). Each

11 deprotection and coupling reaction were performed under microwave energy and nitrogen bubbling.

12 Microwave cycle was characterized by one deprotection step for 60 s at 90°C, three successive washings

13 with 5 mL DMF followed by a double 120 s coupling at 90°C. After peptide assembly, the peptide-resin was

14 washed with DMF and CH_2Cl_2.

15   TAMRA labelling of the peptide was performed by overnight coupling with 1.5 eq. 5(6)-

16 carboxytetramethylrhodamine (Novabiochem), 1.6 eq. HATU and 2 eq. DIEA (Merck) in DMF, then washing

17 with DMF and CH_2Cl_2.

18   Peptide cleavage from the resin and deprotection of the amino acids side chains were carried out with

19 $TFA/H_2O/TIS$ solution (94:3:3 v/v/v) for 3 h at room temperature. The resins were washed with TFA and

20 the filtrates were partially evaporated. Crude peptides were precipitated with cold diethyl ether, collected

21 by centrifugation, dissolved in H_2O/CH_3CN then lyophilized.

22   Unlabeled and TAMRA-labeled peptides were purified by preparative RP-HPLC (Gilson, model PLC 2050

23 equipped with a diode array detector, Waters) using a Atlantis Prep T3 OBD (5 µm, 100 x 19 mm) column

24 (Waters) at 20 mL/min. Peptide identity and purity was checked by LC-MS (Waters). In both cases the

25 solvent system used was: A (0.1 % TFA in H_2O) and B (0.1 % in CH_3CN). All peptides (unlabeled and TAMRA-

26 labeled) were used with a purity higher than 95%.

27

28 **LDH assay:**

29 Caco-2 cells were seeded in 96-well cell culture plates and cultured in DMEM 4.5 g/L glucose supplemented

30 with UltraGlutamine (Lonza), 20% fetal bovine serum (FBS from PAA), 1% MEM non-essential amino acids,

31 1% penicillin/streptomycin, 1% sodium pyruvate and 1% sodium bicarbonate (all 100x, Life Technologies).

32 Afterwards, they were rinsed twice with D-PBS (Life Technologies) and incubated with 200 µL of 1 µM

33 TAMRA-labeled peptides in OptiMEM (Life Technologies) for 24 hours at 37°C and 5 % CO_2. Evaluation of

34 cytotoxicity induced by the CPP-conjugates was performed using Cytotoxicity Detection KitPlus (LDH,

35 Roche Diagnostics) following the manufacturer instructions. After the peptide incubation, at least one well

36 is used as LDH positive control (100% toxicity) by adding Triton X-100 (Sigma-Aldrich) to a final

37 concentration of 0.1% (~15 min incubation at 37°C). Afterwards, 50 µL supernatant of each well were

38 transferred in a new clear 96-well plate. 50 µL of the "dye solution/catalyst" mixture were added to the

39 supernatant and incubated in the darkness for 15 min at room temperature before measuring the

40 absorption at 490 nm. Relative toxicity (%) = [(exp. value – value non-treated cells) / (value triton – value

41 non-treated cells)] x 100.

42

43

Liposome preparation:

2   The following lipids (Avanti Polar Lipids) were used to mimic plasma membrane composition:

3   dioleoylphosphatidylcholine (DOPC) / sphingomyeline (SM) / cholesterol (Chol) (4:4:2; mol/mol/mol).

4   Lipids were dissolved in a 3:1 chloroform/methanol mixture (v/v) at a stock concentration of 25 mg/mL

5   and gently mixed. Lipids were mixed in a round-bottom flask then large unilamellar vesicles (LUV) were

6   prepared by removing organic solvent (evaporation under vacuum for 45-60 min at 80°C).

7   *For TAMRA-LUV quenching:* The lipids were hydrated in milliQ water. The suspension was vigorously

8   agitated with a Vortex (30 s), freeze-thawed 5 times and then extruded 21 times through two stacked

9   100 nm polycarbonate filters (Nucleopore, Whatman).

10   *For leakage assay:* The lipids were hydrated in a buffer (20 mM HEPES, 75 mM NaCl, pH 7.4) containing

11   12.5 mM ANTS fluorescent dye (8-aminonaphthalene-1,3,6-trisulfonic acid, disodium salt; Invitrogen)

12   together with 45 mM DPX quencher (*p*-xylene-bispyridinium bromide; Invitrogen). The suspension was

13   vigorously agitated with a Vortex (30 s), freeze-thawed 5 times and then extruded 21 times through two

14   stacked 100 nm polycarbonate filters. Free dye and quencher were removed by gel filtration on a PD-10

15   desalting column (Amersham Biosciences).

16   LUV concentration was assessed using the LabAssay Phospholipid kit (Wako) as described by the

17   manufacturer and LUV mean size was confirmed by dynamic light scattering (NanoZS, Malvern).

18

19   **Preparation of the cell lysate solution:**

20   Human epithelial colorectal adenocarcinoma (Caco-2) cells were purchased from ATCC (HTB-37). Cells

21   were maintained in DMEM 4.5 g/L glucose supplemented with UltraGlutamine (Lonza), 20% fetal bovine

22   serum (FBS from PAA), 1% MEM non-essential amino acids, 1% penicillin/streptomycin, 1% sodium

23   pyruvate and 1% sodium bicarbonate (all 100x, Life Technologies).

24   For the cell lysate solution preparation, Caco-2 cells were seeded in a T175 flask (Falcon). Until reaching

25   80% of confluence, cells were washed twice with D-PBS (Life Technologies) and trypsinated (0.05%, Life

26   Technologies) for detachment. After a centrifugation step, cells were counted and re-suspended with RIPA

27   buffer (50 mM Tris (Sigma-Aldrich), 150 mM NaCl (Sigma-Aldrich), 1% (v/v) Triton X-100 (Euromedex), 0.1%

28   (w/v) sodium dodecylsulfate (SDS, Sigma-Aldrich), pH 8.0) complemented with 10% Sigmafast® protease

29   inhibitor (Sigma-Aldrich) to a final concentration of 2,000 cells/µL RIPA buffer. This concentration

30   corresponds to that used in 24-well plate fluorescence spectroscopy experiments. Three independent

31   cultures were used for three independent peptide dilutions (see **Figure 4A**)

32

2
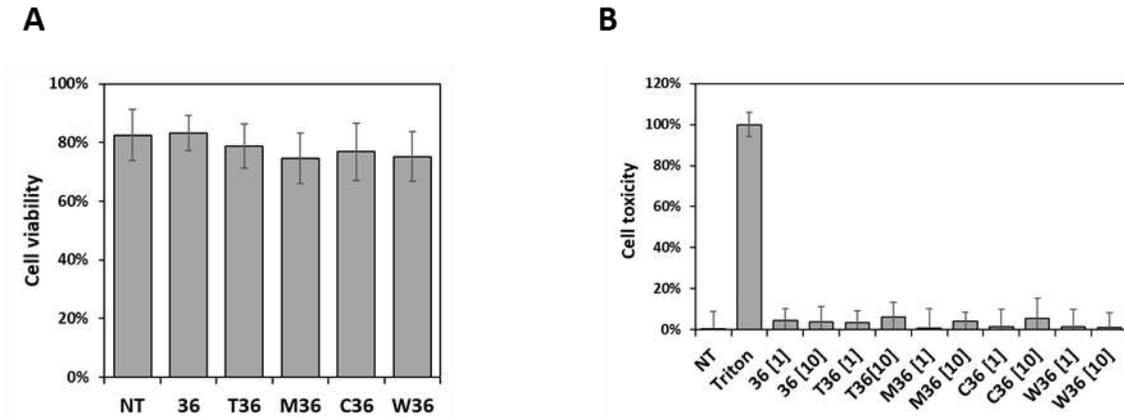
3
4   **Figure S1. Cell viability evaluation after CPP-iCAL36 incubation.**
5   (**A**) Caco-2 cells were incubated with 1 µM TAMRA-labelled peptide solution in OptiMEM for 1.5 h. After
6   cell trypsinization (to remove external peptide), cell viability was assessed by an incubation with the DAPI
7   dye which only labels dead cells. DAPI internalization was recorded by flow cytometry. We observed that
8   the control condition corresponding to non-treated cells (NT) revealed a viability of 80%. A 100% cell
9   viability was not achieved due to post-incubation cell treatents (cell washing, trypsinization, centrifugation
10   and transfer to the flow cytometer on ice) as described in the Materials and Methods section. The peptide-
11   incubated cells, which underwent the same treatments, showed the same viability of 80% showing that
12   the peptide incubation did not affect the cell viability.
13   (**B**) Caco-2 cells were incubated with 1 µM or 10 µM CPP-iCAL36 solutions in OptiMEM for 24 h.
14   Supernatants of each condition were used to quantify cytotoxicity using the LDH assay. None of the CPP-
15   iCAL36 conjugates did induced any particular cytotoxicity, as all values were below 10%.
16   Graphs (A and B) represent the mean of >3 independent experiments. * TAMRA-peptide labeling. 36 =
17   iCAL36, T36 = Tat-iCAL36, M36 = MPG-iCAL36, C36 = C6M1-iCAL36 and W36 = WRAP5-iCAL36.
18   The graphs (A and B) represent the mean $\pm$ SD from n $\geq$ 3 independent experiments measured in
19   duplicates.

20

1
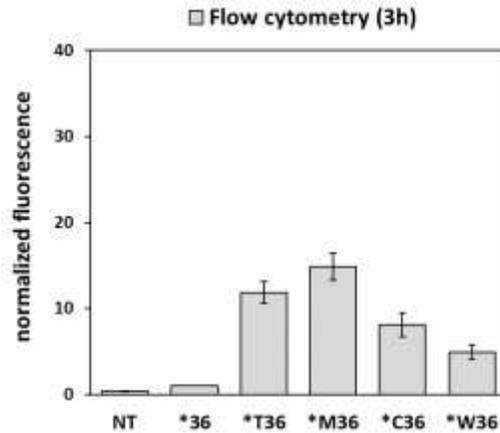
**Figure S2: Comparison of the internalization of TAMRA-labeled CPP-iCAL36 conjugates measured by flow cytometry.**

Caco-2 cells were incubated with 1 µM TAMRA-labeled peptide solution in OptiMEM for 3 h. After cell trypsinization (to remove external peptide) the cell suspensions were analyzed by flow cytometry. The measured fluorescence values were normalized to *iCAL36 (= 1).

The graph represents the mean ± SD from n ≥ 3 independent experiments measured in duplicates. * indicates TAMRA alone or TAMRA-labeling of the peptide. 36 = iCAL36, T36 = Tat-iCAL36, M36 = MPG-iCAL36, C36 = C6M1-iCAL36 and W36 = WRAP5-iCAL36.
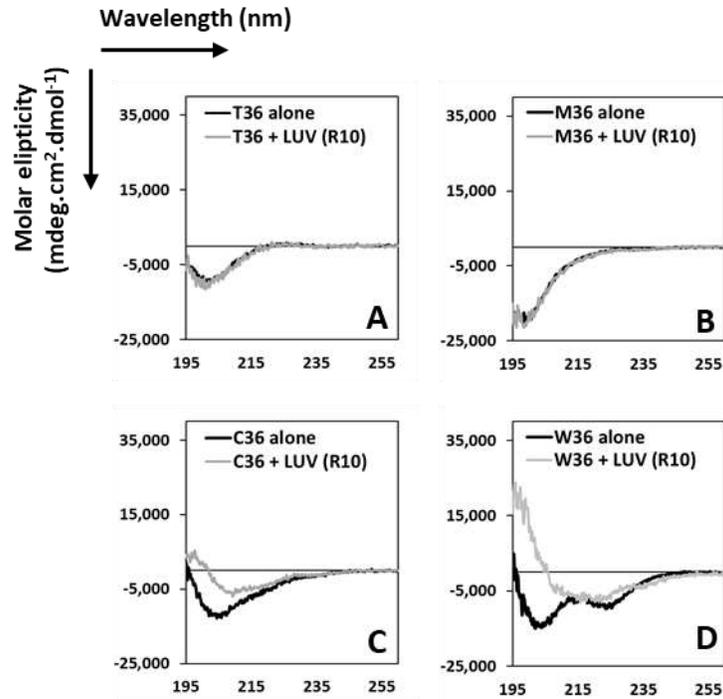
Figure S3. Characterization of the CPP-iCAL36 conformational changes in the presence of LUVs.
Far-UV CD spectra of Tat-iCAL36 (A), MPG-iCAL36 (B), C6M1-iCAL36 (C) and WRAP5-iCAL36 (D) were measured in the absence (black line) or in the presence of LUVs (molar ratio of 10) (grey line).
Secondary structures of Tat-iCAL36 and MPG-iCAL36 are not changed based on LUV addition, whereas the secondary structures of C6M1-iCAL36 and WRAP5-iCAL36 are shifted to a higher amount of alpha helical components.
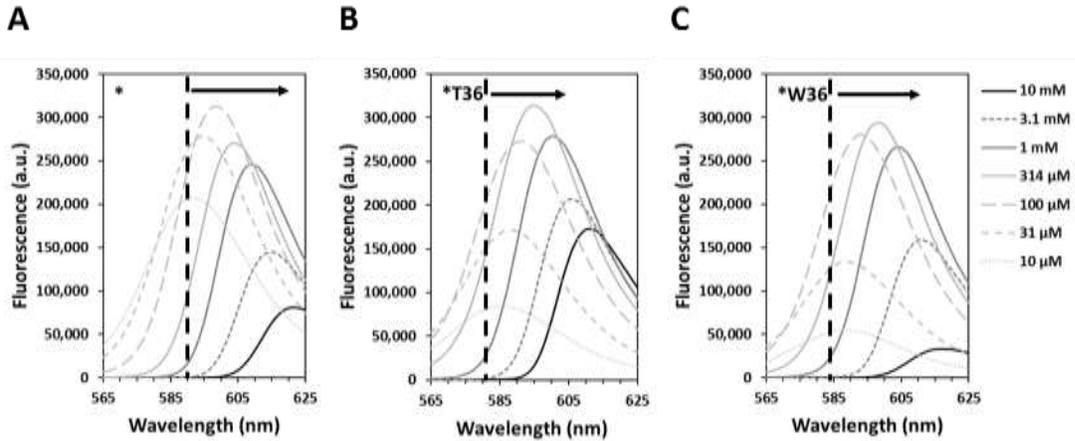
Figure S4. Evaluation of the TAMRA dye properties depending on the peptide concentration.

Representative fluorescence spectra of TAMRA dye alone (**A**), TAMRA labelled Tat-iCAL36 (**B**) and WRAP5-iCAL36 (**C**) measured at concentrations between 10 µM and 10 mM.

Graphs (A, B and C) represent the mean of 2 independent experiments. * indicates the TAMRA dye alone and TAMRA-peptide labeling. T36 = Tat-iCAL36 and W36 = WRAP5-iCAL36. Dotted line correspond to the fluorescence intensity maxima for each compound at 10 µM and the arrow showed the red shift.